International Journal of Mechanics and Energy (IJME)
Vol. 4, Issue 1, 2016, ISSN: 2286-5845

The combined effects of the ratio between the cross heat fluxes and the thermo-dependency parameter on free convection in a square cavity filled with a shear thinning

Mourad Kaddiri [1]*, Mohamed Naimi [1], Abdelghani Raji [1], Mohammed Hassnaoui [2]

[1]*Sultan Moulay Slimane University, Faculty of Sciences and Technologies, Laboratory of flows and Transfers Modeling (LAMET), B.P. 523, Beni-Mellal, Morocco*

[2]*Cadi Ayyad University, Faculty of Sciences Semlalia, Laboratory of Fluid Mechanics and Energetics (LMFE), B.P. 2390, Marrakech, Morocco*

Abstract: Two-dimensional steady-state buoyancy driven flows of thermo-dependent shear-thinning power-law fluid confined in a square cavity, submitted to cross uniform heat fluxes, has been conducted numerically using a finite difference technique. The parameters governing the problem are the thermo-dependence number $(0 \le m \le 10)$ and the ratio between the heat flux imposed on the vertical walls and that imposed on the horizontal ones represented by $a\,(0 \le a \le 1)$, while the flow behavior index *n* is fixed at $(n = 0.6)$ and the Rayleigh number at $(Ra = 5.10^3)$. The effects of these parameters on the flow structure and heat transfer characteristics have been analyzed.

Key words: Heat transfer; Natural convection; Non-Newtonian fluids; Numerical study; Square cavity.

Nomenclature

c_1: temperature coefficient.

g: acceleration due to gravity $\left(m/s^2\right)$

H': height or width of the enclosure (m)

k: consistency index for a power-law fluid at the reference temperature $\left(Pa \cdot s^n\right)$

m: thermo-dependence number

n: flow behavior index for a power-law fluid.

Nuh: the horizontal average Nusselt number.

Nuv: the vertical average Nusselt number.

Pr: generalised Prandtl number.

q': constant density of heat flux $\left(W/m^2\right)$

Ra: generalised Rayleigh number.

T: dimensionless temperature, $\left(= (T' - T_r')/\Delta T^*\right)$

T_r': reference temperature (K)

ΔT^*: characteristic temperature $\left(= q'H'/\lambda\right)$ (K)

(u,v) dimensionless horizontal and vertical velocities $\left(= (u',v')/(\alpha/H')\right)$

(x,y) : dimensionless horizontal and vertical coordinates $\left(= (x',y')/H'\right)$

Greek symbols

α : thermal diffusivity of fluid at the reference temperature $\left(m^2/s\right)$

β: thermal expansion coefficient of fluid at the reference temperature $\left(1/K\right)$

λ: thermal conductivity of fluid at the reference temperature $\left(W/m \cdot °C\right)$

μ: dynamic viscosity for a Newtonian fluid at the reference temperature $\left(Pa \cdot s\right)$

μ_a : dimensionless effective viscosity of fluid.

ρ: density of fluid at the reference temperature $\left(kg/m^3\right)$

Ω: dimensionless vorticity, $\left(= \Omega'/\left(\alpha/H'^2\right)\right)$

ψ : dimensionless stream function, $\left(= \psi'/\alpha\right)$

Superscript

': dimensional variables

Subscripts

a: effective variable

max: maximum value

r: reference value taken at the cavity centre

*** Corresponding author:** Mourad Kaddiri
E-mail: mouradkadiri@usms.ma

1. Introduction

Natural convection in Newtonian and non-Newtonian fluids in closed rectangular cavities has been studied using numerical simulations and experiments, owing to the practical importance of such configurations in many engineering applications (papermaking, oil drilling, slurry transporting, food processing, polymer). Although the case of Newtonian liquid has been thoroughly investigated (see Gebhart et al. [1] for example). The studies number reported on natural convection involving non-Newtonian fluids has been increased during the last two decades [2], but owing to their complex rheological behavior and their particular isothermal or non-isothermal flow conditions more investigations are to be undertaken in this area.

Most of the works conducted in the past have been substantially oriented to study unidirectional heat transfers resulting from imposed temperature gradients (due to heat fluxes or temperature differences) either parallel or normal to gravity.

In some practical situations, much more complex boundary conditions may be encountered where horizontal and vertical temperature gradients could be simultaneously imposed across the cavity.

Another challenging problem is the dependence of the rheological properties of these fluids on the temperature. To our best knowledge, most of the reported studies on natural convection in non-Newtonian fluids ignore such an aspect. This can be a serious assumption, since in many cases this effect has a significant influence on heat transfer [3]. Therefore, this work is a numerical contribution to the study of the thermo-dependence effects on buoyancy convection heat transfer in a square cavity filled with a shear thinning and submitted to across heat fluxes.

2. Mathematical formulation and solution procedure

2.1 Problem statement and viscosity model

The geometry under consideration is sketched in Figure (1). It consists of a two-dimensional square enclosure of size $H' \times H'$ subjected to cross uniform densities of heat flux, q' and aq'.

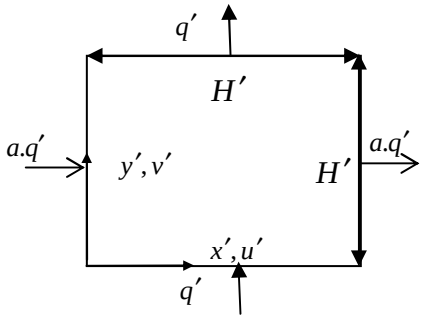

Figure 1. Sketch of the geometry and coordinates system

The non-Newtonian fluids considered here are those whose rheological behaviors can be approached by the power-law model, due to Ostwald-de Waele, which, in terms of laminar effective viscosity, can be written as follows:

$$\mu_a' = k_T \left(2\left(\left(\frac{\partial u'}{\partial x'} \right)^2 + \left(\frac{\partial v'}{\partial y'} \right)^2 \right) + \left(\frac{\partial u'}{\partial y'} + \frac{\partial v'}{\partial x'} \right)^2 \right)^{\frac{n_T - 1}{2}} \quad (1)$$

The two empirical parameters n_T and k_T, appearing in equation (1), are the flow behavior and consistency indices, respectively. They are, in general, functions of the temperature, but in most of cases the temperature-dependence of n_T can be ignored $(n_T = n)$ since it is weak compared to that of k_T [3,4], which is described by the Frank-Kamenetski exponential law [5]:

$$k_T = k e^{-c_1 (T' - T_r')} \quad (2)$$

reflecting the viscosity diminution with the temperature, where c_1 is an exponent related to the flow energy activation and the universal gas constant, and T_r' is a reference temperature.

Note that for $n=1$ the behavior is Newtonian and the consistency is just the viscosity. For $0<n<1$, the effective viscosity decreases with the amount of deformation and the behavior is shear-thinning. Conversely, for $n>1$, the viscosity increases with the amount of shearing, which implies that, the fluid behavior is shear-thickening.

2.2 Governing equations and boundary conditions.

On the basis of the assumptions commonly adopted in natural convection problems and using the characteristic scales H', H'^2/α, α/H', α/H'^2, $q'H'/\lambda$ and α, which correspond respectively to length, time, velocity, vorticity, temperature and stream function, the dimensionless governing equations for Boussinsq-temperature-dependent viscosity fluids, written in terms of vorticity, Ω, temperature, T, and stream function, ψ, are as follows:

$$\frac{\partial \Omega}{\partial t}+\frac{\partial (u\Omega)}{\partial x}+\frac{\partial (v\Omega)}{\partial y}= \Pr\left[\mu_a\left[\frac{\partial^2\Omega}{\partial x^2}+\frac{\partial^2\Omega}{\partial y^2}\right]+2\left[\frac{\partial \mu_a}{\partial x}\frac{\partial \Omega}{\partial x}+\frac{\partial \mu_a}{\partial y}\frac{\partial \Omega}{\partial y}\right]\right] + S_\Omega \tag{3}$$

$$\frac{\partial T}{\partial t}+\frac{\partial (uT)}{\partial x}+\frac{\partial (vT)}{\partial y}=\frac{\partial^2 T}{\partial x^2}+\frac{\partial^2 T}{\partial y^2} \tag{4}$$

and

$$\frac{\partial^2 \psi}{\partial x^2}+\frac{\partial^2 \psi}{\partial y^2}=-\Omega \tag{5}$$

where

$$u=\frac{\partial \psi}{\partial y};\ v=-\frac{\partial \psi}{\partial x};\ \Omega=\frac{\partial v}{\partial x}-\frac{\partial u}{\partial y} \tag{6}$$

$$\mu_a=e^{-mT}\left[2\left[\left(\frac{\partial u}{\partial x}\right)^2+\left(\frac{\partial v}{\partial y}\right)^2\right]+\left[\frac{\partial u}{\partial y}+\frac{\partial v}{\partial x}\right]^2\right]^{\frac{n-1}{2}} \tag{7}$$

and

$$S_\Omega=\Pr\left[\left[\frac{\partial^2\mu_a}{\partial x^2}-\frac{\partial^2\mu_a}{\partial y^2}\right]\left[\frac{\partial u}{\partial y}+\frac{\partial v}{\partial x}\right]-2\frac{\partial^2\mu_a}{\partial x\partial y}\left[\frac{\partial u}{\partial x}-\frac{\partial v}{\partial y}\right]\right] + \Pr Ra\frac{\partial T}{\partial x} \tag{8}$$

For the present problem, the appropriate non-dimensional boundary conditions are:

$$u=v=\psi=\frac{\partial T}{\partial x}+a=0 \quad \text{for } x=0 \text{ and } 1 \tag{9}$$

$$u=v=\psi=\frac{\partial T}{\partial y}+1=0 \quad \text{for } y=0 \text{ and } 1 \tag{10}$$

Note that the major disadvantage of this formulation lies in the fact that Ω is unknown at the boundaries. To overcome such a difficulty, the Woods formulation has been adopted for stability and accuracy reasons [6].

2.3 Governing parameters

In addition to the flow behaviour index, *n*, three other dimensionless parameters appear in the governing equations. These are the Pearson, Prandtl and Rayleigh numbers defined, respectively, as:

$$m=-\frac{1}{k_T}\frac{dk_T}{\mathrm{dT}}=-\frac{d\ln(k_T/k)}{\mathrm{dT}}\ ,\qquad \Pr=\frac{(k/\rho)H'^{2-2n}}{\alpha^{2-n}} \tag{11}$$

and $\quad Ra=\dfrac{g\,\beta\,H'^{2n+2}q'}{(k/\rho)\alpha^n\,\lambda}$

The Pearson number [7], which is a new dimensionless quantity taking place in this study, measures the effect of temperature change on the effective viscosity.

2.4 Heat transfer

The steady solution has been used to calculate the average Nusselt number in the horizontal and vertical directions, respectively, defined as:

$$Nu_h=\frac{q'H'}{\lambda\overline{\Delta T_v'}}=\frac{a}{\overline{\Delta T_v}} \tag{12}$$

$$Nu_v=\frac{bq'H'}{\lambda\overline{\Delta T_h'}}=\frac{1}{\overline{\Delta T_h}} \tag{13}$$

where $\overline{\Delta T_v}$ is the average temperature difference between the two vertical walls and $\overline{\Delta T_h}$ is the average temperature difference between the two horizontal walls.

2.5 Heatlines formulation

The visualization of the paths followed by the heat flow through the enclosure requires the use of the heatlines concept, which consists of lines of constant heat function, *H*, that are defined, according to Kimura and Bejan [8], from the following equations

$$\frac{\partial H}{\partial y} = uT - \frac{\partial T}{\partial x};\quad -\frac{\partial H}{\partial x} = vT - \frac{\partial T}{\partial y} \tag{14}$$

whose derivation, with respect to *x* and *y*, and combination give rise to

$$\frac{\partial^2 H}{\partial x^2} + \frac{\partial^2 H}{\partial y^2} = -\frac{\partial vT}{\partial x} + \frac{\partial uT}{\partial y} \tag{15}$$

To obtain the boundary conditions associated with equation (15), an integration of equation (14), along the four cavity walls, is necessary, which gives:

$$H(0,y) = H(0,0) \quad \text{for} \quad x = 0 \tag{16}$$

$$H(x,1) = H(0,1) - x \quad \text{for} \quad y = 1 \tag{17}$$

$$H(1,y) = H(1,1) \quad \text{for} \quad x = 1 \tag{18}$$

$$H(x,0) = H(1,0) + 1 - x \quad \text{for} \quad y = 0 \tag{19}$$

Finally, the solution of equation (15) yields the values of *H*, in the computational domain, whose contour plots provide the heatline patterns. Note that only the differences between the values of *H* are required instead of its intrinsic ones, which offers the possibility to choose $H(0,0) = 0$ as an arbitrary reference value for *H*.

2.6 Solution procedure

The two-dimensional governing equations have been discretized using the second order central finite difference methodology with a regular mesh size. The integration of equations (3) and (4) has been performed with the Alternating Direction Implicit method (ADI), originally used for Newtonian fluids and successfully experimented for non-Newtonian power-law fluids [9-11]. To satisfy the mass conservation, equation (5) has been solved by a Point Successive Over Relaxation method (PSOR) with an optimum relaxation factor calculated by the Frankel formula [6]. A grid of 81×81 has been required for obtaining adequate results. At each time step, δt, which has been chosen between 10^{-7} and 10^{-4} (depending on the values of the parameters *a* and *m*), the convergence criterion $\sum_{i,j}\left|\psi_{i,j}^{k+1} - \psi_{i,j}^{k}\right| \Big/ \sum_{i,j}\left|\psi_{i,j}^{k+1}\right| < 10^{-4}$ has been satisfied for ψ, where $\psi_{i,j}^{k}$ is the value of the stream function at the node (i,j) for the k[th] iteration level.

3. Results and discussion

As was reported in the past by [11], the convection is rather insensitive to *Pr* variations, provided that this parameter is large enough as it is the case for the non-Newtonian fluids and for a large category of fluids having a Newtonian behavior. Therefore, *Pr* is not considered as an influencing parameter in this study and the simulations are conducted with $Pr \to \infty$, i.e. by neglecting the inertia terms on the left hand side of equation (3) owing to their negligible contribution. To examine the cross fluxes and the thermo-dependency effects, some results, corresponding to *a* = 0, 0.2, 0.5, 0.7 and 1, *m* = 0 and *m* = 10, *n* = 0.6 and *Ra* = 5×10³, are presented and discussed.

Hence, as can be seen from figure (2), displaying streamlines (left), isotherms (middle) and heatlines (right), the unicellular nature of the flow undergoes significant changes, for all the values of *a*, when *m* passes from 0 to 10. In fact, the streamlines lose their centro-symmetry and become more crowded near the hot walls, giving rise to a stagnation zone which tends to be reduced near the upper wall and to be extended next to the right one with an increasing *a*, while for, the effect of *a* is such that the streamlines become almost parallel to the central part of each wall.

As for the isotherms, they seem to be closely spaced and less distorted in the stagnation region when *m* passes from 0 to 10, depending on *a*, whose increase leads to their rotation in the clockwise direction.

On the other hand, in order to have a microscopic description of the heat transfer process, which is different from the conventional Nusselt number that describes macroscopically such a phenomenon, a heatlines analysis is required. Hence, with comparison to the iso-consistent case ($m = 0$), the heatlines corresponding to the case *m* = 10 present more distortion, which indicates that the path followed by the heat flow to reach the cold wall is more complicated in the rheological sub-layer. Therefore, the heat transfer is expected to be deteriorated in such a situation. Like the isotherms, an increase of *a* leads to a deviation of the heatlines in the clockwise direction whatever the value of *m*.

Moreover, figures (3) and (4), in which are depicted the variations of Nu_h and Nu_v , show that these quantities increase with *a*. However, if figure (3) indicates a degradation of heat transfer in the horizontal direction with *m* ($Nu_h\,(\mathrm{m}=0) > Nu_h\,(\mathrm{m}=10)$, which takes more importance while increasing *a*, figure (4) informs the about the same effect of *m* on heat transfer in the vertical direction until a critical value a_c beyond which an opposite effect is observed, i.e. ($Nu_v\,(\mathrm{m}=0) < Nu_v\,(\mathrm{m}=10)$.

4. Conclusion

A numerical study of the steady thermal convection in a square enclosure filled with shear-thinning power law fluid and submitted to cross uniform heat fluxes is carried out. The case of the variation of viscosity with temperature has been taken into account. Results on the flow and thermal fields are derived from the combined study of control parameters. It appears that the thermo-dependent behavior affects many natural convection in terms of flow and heat transfer and depending on the proportion of the cross heat fluxes.

Références

[1] B. Gebhart, Y. Jaluria, R. L. Mahajan, and B. Sammakia, Buoyancy-induced flows and transport, chap. 16, Hemisphere, Washington, DC, 1988.

[2] Mi. Ohta, Ma. Ohta, M. Akiyoshi and E. Obata, A numerical study on natural convective heat transfer of pseudoplastic fluids in a square cavity, Num. Heat Transfer Part A, Volume 41, pages 357-372, 2002.

[3] C. Nouar, Thermal convection for a thermo-dependent yield stress fluid in an axisymmetric horizontal duct, Int. J. heat Mass Transfer, Volume 48, pages 5520-5535, 2005.

[4] V. Scirocco, R. Devienne, and M. Lebouché, Ecoulement laminaire et transfert de chaleur pour un fluide pseudo-plastique dans la zone d'entrée d'un tube, Int. J. Heat Mass Transfer, volume 28(1), pages 91-99, 1985.

[5] V.S. Solomatov, and A.C. Barr, Onset of convection in fluids with strongly temperature-dependent power-law viscosity, Physics of the Earth and Planetary Interiors, volume 155, pages 140-145, 2006.

[6] P.J. Roache, Computational Fluid Dynamics, New Mexico: Hermosa Publishers, 1982.

[7] C. Métivier, C. Nouar, Linear stability of the Rayleigh–Bénard Poiseuille flow for thermodependent viscoplastic fluids, Journal of Non-Newtonian Fluid Mechanics, volume 163, pages 1-8, 2009.

[8] S. Kimura and A. Bejan, The Heatline Visualization of Convective Heat Transfer, ASME Journal of Heat Transfer, volume 105, pages 916–919, 1983.

[9] S Turki, Contribution to Numerical Study of Natural and Mixed Convection Heat Transfers in Confined Non-Newtonian Fluids, Ph.D. Thesis, CNAM, Paris, France, 1990.

[10] H. Ozoe, and S.W. Churchill, Hydrodynamic stability and natural convection in Ostwald–De Waele and Ellis fluids: the development of a numerical solution, AIChE J., volume 18, pages 1196-1207, 1972.

[11] M. Lamsaadi, M. Naïmi, and M. Hasnaoui, Natural convection of non-Newtonian power-law fluids in a shallow horizontal rectangular enclosure uniformly heated from the side, Energy Conversion and Management, volume 47, pages 2535-2551, 2006.

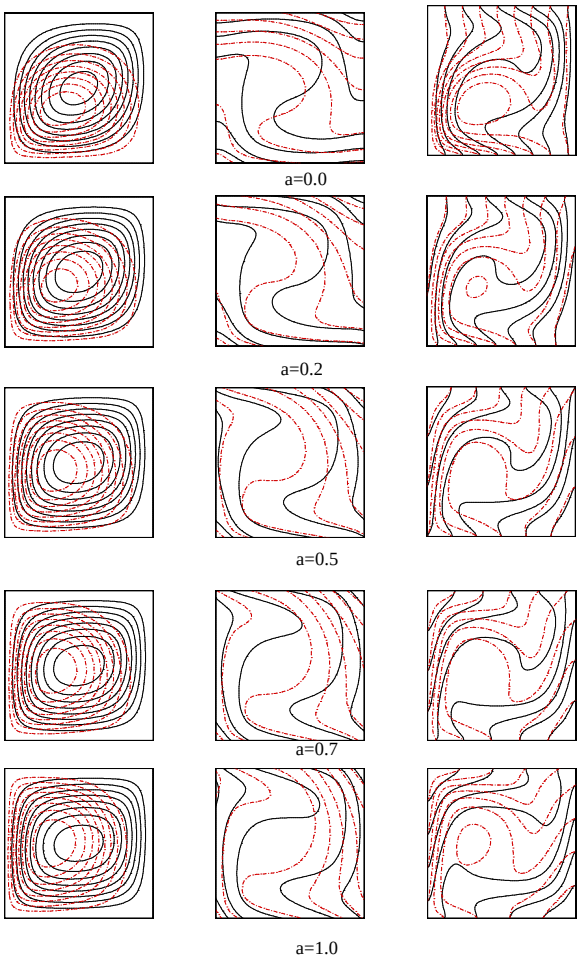

Figure 2. Streamlines (left), isotherms (medium) and heatlines (right) for $Ra = 5.10^3$, $n = 0.6$ **and** $m = 0$ **(black solid line),** $m = 10$ **(red dashdot line) and various value of *a*.**

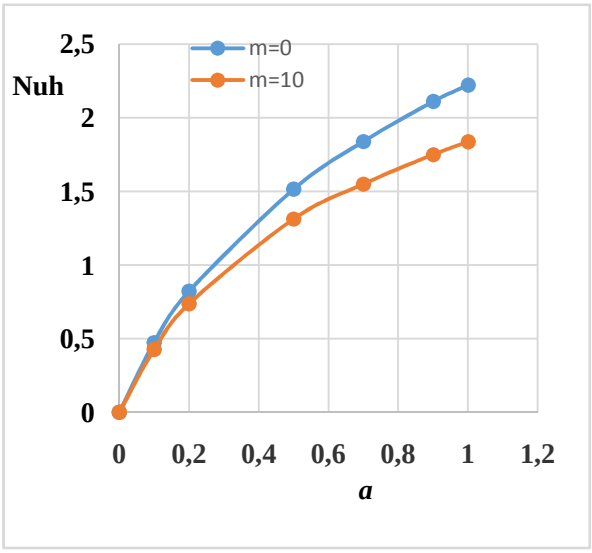

Figure 3. Evolution of the average horizontal Nusselt number with *a*, for $Ra = 5.10^3$, $n = 0.6$, $m = 0$ **and** $m = 10$.

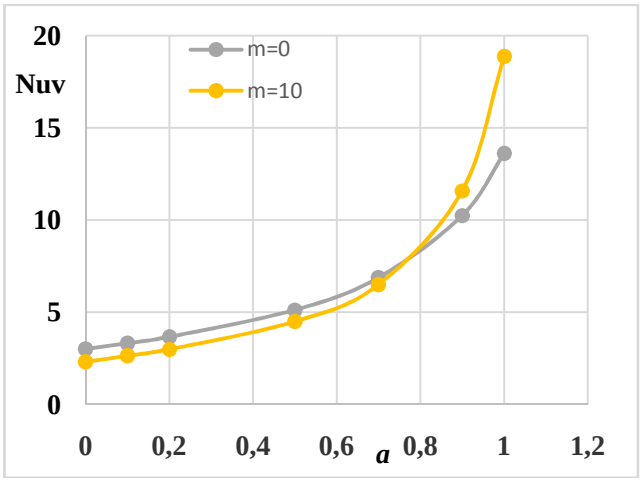

Figure 4. Evolution of the average vertical Nusselt number with *a*, for $Ra = 5.10^3$, $n = 0.6$, $m = 0$ **and** $m = 10$.